Early Scavenger Dimensioning in Wireless Industrial Monitoring Applications

Borja Martinez, *Member, IEEE*, Màrius Montón, *Member, IEEE*, Ignasi Vilajosana,
and Xavier Vilajosana, *Senior Member, IEEE*

Abstract—The Industrial Internet era is pushing for even more miniaturized, powerful and energy efficient devices that seamlessly integrate to the Internet and aim to improve efficiency of industries by monitoring, actuating or sampling data from machines, infrastructures and systems. Industrial low power wireless protocols are one of the key enablers of that revolution but still energy consumption is what is limiting ubiquitous deployments of perpetual and unattended devices. The adoption of energy harvesting technologies is enabling autonomously powered control and monitoring systems on Industries, Infrastructures and Cities. Yet putting these systems together require a clear understanding of their capabilities and behavior in order to dimension their energy needs and to contribute to the development of a new generation of self-powered ubiquitous devices. Therefore, this article discusses, through a use case, the trade-off to reliably dimension scavenger properties to network requirements and application needs, with the main objective to enable Industries to optimize the adoption of that technologies while keeping low technical risks.

Index Terms—Low-power modelling, industrial wireless, energy scavenging, self-powered wireless sensor networks.

I. INTRODUCTION

INDUSTRIES are shifting to the use of wireless sensing and actuating technologies to improve their productivity, energy efficiency, and/or to develop new products and services [1]. In this shift, a key enabler is the development of a new generation of wireless devices that consume less energy, which is being driven by new microcontrollers, new radio technologies, new communication standards [2], [3] and enhancements to sensing and actuating peripherals. These features, added to the ability to seamlessly communicate over the Internet [4], boosted the possibility to gather an unprecedented amount of data, and lead to the emergence of numerous sensing and actuation applications [5] [6]. Clear examples are the emergence of the industry of wearable devices for health applications [7], smart cities pervasive instrumentalization [8] or the improvement of actuation and monitoring systems in the oil and gas industries.

However, making more energy efficient technologies is still far from having those envisaged ubiquitous deployments (so called the Internet of Things [9] [10]), which will enable

B. Martinez is with Universidad Autonoma de Barcelona (UAB), Spain and Worldsensing, Barcelona, Spain. (e-mail: borja.martinez@uab.cat)

M. Montón is with University Autonomous of Barcelona, Bellaterra, Spain and IoT-Parteners, Barcelona, Spain

I. Vilajosana is Worldsensing, Barcelona, Spain.

X. Vilajosana is with Universitat Oberta de Catalunya (UOC), Spain and Worldsensing, Barcelona, Spain.

optimal industrial operation, or will contribute to improve the social welfare. Viable systems, especially for industry, are those whose operational costs enable fast returns on investment, even when deployed at a large scale. Clear enablers are a) harvesting technologies [11], since they render those devices to be (almost) self-powered; and b) emergent low power industrial wireless standards and technologies [12], [13], [14], which provide IP connectivity (compatibility and interoperability) while ensuring deterministic communication. It is therefore logical that industry is demanding wireless sensing equipment to be (almost) self-powered [15] [16] [17]. Yet, today, it is possible to build a device which features this industrial wireless performance [18][19], being able to in-node analyze the acquired data. However, energy-dimensioning the device in order for it to meet the application requirements, while retaining this wireless reliability, is not something straightforward.

Note that to develop extremely low power self-sustainable devices, a system-wide characterization and optimization is fundamental for the development of the device at a reasonable cost, requiring to the system designer to carefully plan the energy consumption [20]. In most of the applications, designs are guided by worst case scenarios for hardware energy consumption [21], i.e. application designers usually do not consider that different tasks conforming the application, despite of running concurrently, follow significantly different rates in their duty-cycles). In this article we *claim* that a clear understanding of the dependence on the different application parameters, their interrelations, and the identification of periodic tasks that compose the application, are essential for an efficient energy management.

Thus, this article advises on how to early estimate the energy consumption of the application in a realistic way. With this aim, we illustrate through a use case a method to aid engineers in understanding the energy life-cycle within the application, which will enable them to determine tolerance margins and trade-offs.

The use case proposed, on which vibrational sensing devices are used to perform in-node modal analysis of an infrastructure, and on which an emerging low power long range wireless technology is used to connect the infrastructure to the Internet [22], is motivated by the fact that frequency measurements are central to multiple industries. Vibrational sensors are used to perform modal and harmonic analysis of the vibration of motors, infrastructures, etc, which is fundamental to determine the health of the machinery [23] or some infrastructure [24]. For this scenario, harvesting technologies are mature enough

in order to be cost-effectively deployed. Thus we pay special attention to the early dimensioning of the scavenger according to the expected energy income, while accounting with the network, sampling and processing requirements and mechanical constrains.

The article is organized as follows. First, Section II briefly presents a real IoT application as our case study. Then, in Section III the article derives a general methodology from the presented use case. In Section IV we go further with our example and discuss about the correct dimensioning of a self-sustainable application and address the problem of discontinuous sources of energy, before concluding in Section V.

II. An IoT Case Study: Monitoring Power Line Towers

The main reasons for power transmission tower failure can be attributed to structural damage due to corrosion, mechanical damage caused by impacts, strong winds or structural overloading due to ice and snow on the conductor lines. If the structure begins to deteriorate, corrosion advances exponentially and in a few years can oxidize the tower to the point of failure. Furthermore, small structural damages, such as the destruction of small traversal bars or the bending of some structural elements of the tower, produce local defects that can also cause the tower collapse. Critically, as the tower deterioration accelerates, the repair time, labor and materials cost to repair the tower increase significantly [25]. The periodic inspection of transmission towers is hence necessary to ensure the reliability of electric service to customers. Ground inspections during the last 50 years (in the pre-IoT era) have been only performed on a fixed schedule in very specific areas. For this purpose a field engineer drives to a specific tower and inspects every element of the structure. In fact, due to the spread and large number of towers, it is difficult to assess the structural integrity of the entire network from the ground, and it is often necessary to conduct aerial inspections to make a qualitative assessment. In this case, experts grade tower conditions based only on visual assessments, but this method is subjective and very expensive.

In short, quantifying the remaining strength and service life of towers is still today problematic. Servicing companies and utilities will inevitably spend valuable time inspecting towers that would anyway keep functioning for a long time. However, tower failures are very problematic, they produce unplanned downtimes and energy delivery losses, which in turn may affect businesses and population. This sort of problems can be avoided through preventive maintenance at just the right time driven by real-time state of health information.

In the present scenario, we envisage each tower equipped with multiple sensing elements which provide tower's structural state information [26]. A wireless node monitors the health of the tower in real time [27] and solar energy is used to power the device, taking advantage of the solar exposure of towers.
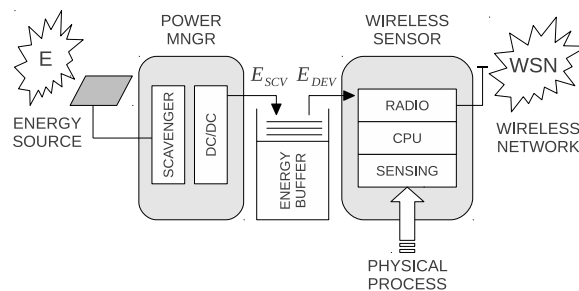

Fig. 1. Generic Self-Powered Wireless Sensor device.

III. Early Power Estimation of Wireless Sensor Devices

The power consumption of *Industrial Wireless Sensor* devices (see Fig. 1) can be easily characterized because they follow a common behavioral pattern. Data is acquired by some sensor of the system, eventually processed in a controller unit and finally some information sent through a wireless channel. This process repeats over time and application's duty cycle is essential to control the energy consumption. The shorter the duty cycle, the lower the average power.

As an example, in our case study, each time the device wakes up three steps are executed: *i)* capture of a set of samples; *ii)* computation of the acceleration spectrum for quantitative analysis; and *iii)* an alarm is triggered only when an anomaly is detected, generating a radio message. In background, low power wireless communication technologies require certain activity. This is because it is necessary to communicate information about the node status and, in our particular case, to keep track of the network synchronization. Fig. 2 shows schematically a temporal sequence of such an application and generalizes our use case. We consider this case to be representative for most of industrial applications, despite of the sensing and communication technologies being used.
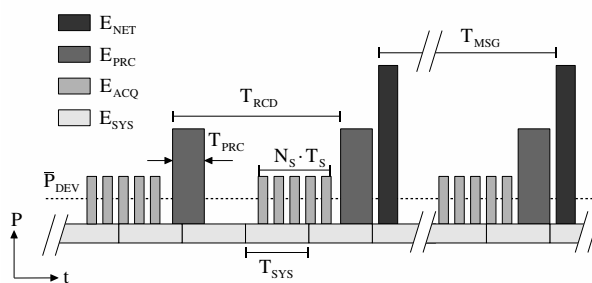

Fig. 2. Characteristic time evolution of energy usage split in different components. The system wakes-up within T_{RCD} intervals, captures a sequence of N_S samples at T_S sampling period, and takes a time T_{PRC} to process the record. The average interval time between radio packets is depicted as T_{MSG}. Dashed line represents the average consumption.

Once determined and characterized the inherent operational cycles of the tasks involved in the application, it becomes necessary to estimate the energy spent within each cycle. Obviously there are different alternatives. We propose here to follow a semi-empiric approach originally presented in [28].

This approach can be summarized as follows: first, the basic blocks are measured experimentally in the real platform; then, a model is built upon this fundamental blocks, on which the energy of each element is averaged over the period of repetition; finally, the total power is obtained as the sum of each individual power contribution.

The characterization of the building blocks is carried out statistically, i.e., taking several measurements of each contribution and then using the fitting results as an input of the proposed model.

A. Industrial Network Energy Consumption Modeling

The network energy consumption is modelled from a two level perspective, that is, from a packet point of view and from a network usage point of view. This entails the understanding of the costs of sending a packet and determining the amount of packets/activity that the application and network generate.

In our use case, we selected a low power wide area network technology developed by Cycleo (now Semtech) which is being widely used in new Industrial and Smart City deployments. The reason of its success can be fundamentally attributed to its extended coverage and reduced network infrastructure requirements. Cycleo operates in the sub GHz ISM band, and the technology is referred as LoRa (Long Range) [22].

1) Packet characterization: LoRa's physical layer achieves very long range and reduced power consumption due to the use of wide-band linear frequency modulated pulses and the use of different spreading factors (i.e., the ratio between chip rate and the symbol rate) to tune the range of the transmissions. The spreading factor increase the sensitivity in the receiver side and thus achieving and extended range, but it also provides a mechanism to modulate energy consumption.

In the case of the Semtech Transceiver, this SF parameter can be configured from SF6 to SF12 (64 to 4096 chips/symbol). This ends with a reduction in bit-ratio that affects the time needed to send the payload, and hence, the power consumed at each transmission [22]. Fig. 3 shows several transmission traces measured with different spreading factors (SF7 & SF12) In this figure, it can be appreciated the significant difference on channel usage.

It turns out that each step in the spreading factor scale doubles the time that radio spends in active state. This suggests that the charge per message can be characterized by an exponential function in the form $\mathcal{H}(N) = \mathcal{O}(h(N)) = 2^N$, leading to Eq. (1) as a tentative fitting function.

$$\bar{Q}_{MSG}^{(N_{SF})} \cong \mathcal{Q}_{PYLD} \cdot 2^{N_{SF}} + \bar{Q}_B \qquad (1)$$

Fig. 4 presents a characterization of the amount of charge used by different spreading factors. In the experiment, the power consumption of each transmission is fitted with a training set of ≈ 100 samples for each modulation. Numerical values obtained are $Q_{PYLD} = 6.1\,\mu C$ and $\bar{Q}_B = 13.0\,\mu C$ (The error bars represent the empirical dispersion obtained). Results show that the model presented is in full agreement with measurements within the experimental error.

Although LoRa is used as a case study, this characterization can be easily applied to other radio technologies. In general,
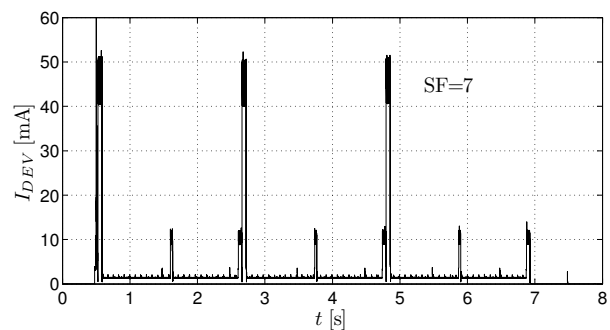
(a) Transmission using Spreading Factor 7
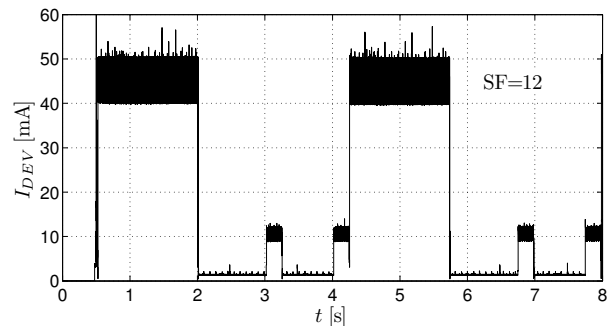
(b) Transmission using Spreading Factor 12

Fig. 3.   Characterization of LoRa transmissions

the key issue is to be able to characterize the consumption of a radio message, which will be used as an input parameter for the next layer. As an example, in [29] and [30] can be found a similar characterization for a Time Synchronized Channel Hopping networks such as WirelessHART or IEEE802.15.4e.
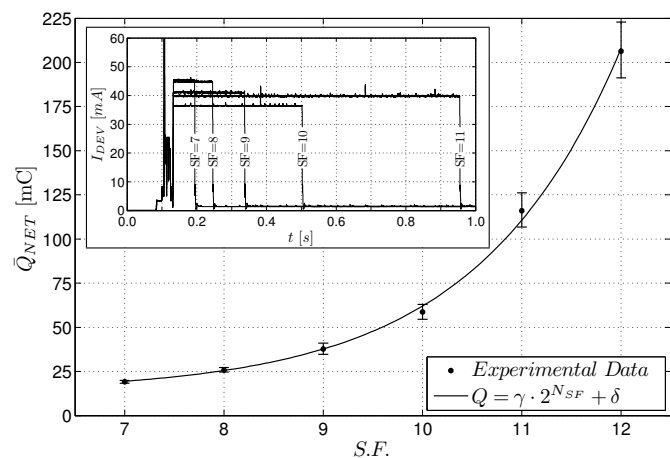

Fig. 4.   Fitting LoRa spreading-factor.

2) Network activity characterization: After understanding the contribution to the energy expenditure of each packet, we are concerned with the amount of messages that are generated during the lifetime of the network to guarantee its reliable operation and to ensure the proper operation of the application. In our approach, LoRa nodes organize in a multi-hop network on which each node keeps track of several best connected neighbors. All nodes in the network operate following a slotted

structure and slot boundaries are kept closely aligned between nodes.

This approach is similar to other Industrial Wireless technologies and, therefore, the presented use case can be extrapolated to most of the standard Industrial network technologies [12], [13].

Due to the low data-rate and to reduce the power consumption, nodes only exchange synchronization messages when required, following an adaptive synchronization mechanism. Basically, each node selects one time source parent in the network to synchronize with and periodically the device aligns its clock with it using a pair-wise communication. Typical interval between synchronization packets is a value around 60 seconds if we assume crystals with a drift of 10ppm [31].
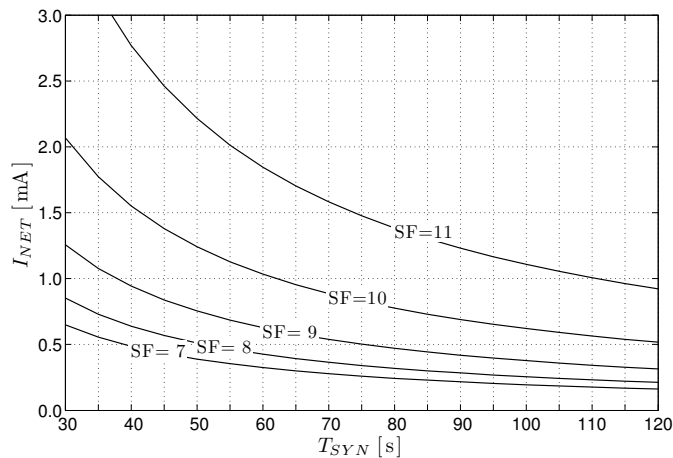

Fig. 5. Influence of time between synchronization messages on device current consumption.

According to this network description, we can determine the average current to keep the network operational by applying Eq. (2):

$$\bar{I}_{NET}^{(N_{SF})} \cong \frac{\bar{Q}_{MSG}^{(N_{SF})}}{T_{SYN}} + \bar{I}_B \qquad (2)$$

In Eq. (2) $\bar{Q}_{MSG}$ represents average charge required per packet for this particular radio technology. T_{SYN} is the average time between synchronization packets. This means that the time between synchronization packet acts as a control parameter for the network energy, giving a characteristic functional dependency $\bar{I}_{NET} \propto 1/T_{SYN}$ (as shown in Fig. 5). In turn, $\bar{I}_B$ accounts for all components standby and quiescent currents. It can be considered a constant value, and in general can be neglected in front of the first member of the equation. Additionally, when measuring in a real platform, a term related with the RTOS management tasks is always present (depicted as I_{SYS} in Fig. 2). This term is a constant bias for all measurements and will be accounted only once in the general model.

3) Application Layer: For this particular case, data messages are only generated when an alarm is triggered, which is an unlikely case. Therefore, the traffic generated by the application layer can be considered negligible. In applications that generate periodic data traffic, a similar expression to

Eq. (2) can be derived, on which a characteristic parameter T_{DAT} would account for the average time between data messages.

B. Data acquisition

The charge drained to record one single sample can be obtained by looking at the number of cycles required by the ADC to capture the sample as well as the cycles required to move the data to memory. Further details on this procedure can be found in [29]. A second alternative is to follow an approach similar to the network fitting presented, i.e, a semi-empirical characterization of the acquisition subsystem.

Independently of the method, an estimation of the charge per sample $\bar{Q}_{SMP}$ is required. Thus, for each record [1] a simple linear dependence with the number of samples acquired is obtained. The average current of the acquisition block is computed dividing the total charge $N_S \cdot \bar{Q}_{SMP}$ by the time elapsed between consecutive records T_{RCD} (Eq. 3), i.e. the wake-up period of the application.

At this point, it is worth noting the following observation regarding the energy control. While in many situations the sampling period T_S is determined by the filtering requirements of the underlying physical process (e.g. AC noise filtering in magnetic readings) the time between consecutive records is scheduled from the application layer, thus providing a control mechanism over the energy consumption at the expense of increasing the monitoring interval time.

$$\bar{I}_{ACQ} \cong \frac{\bar{Q}_{SMP} \cdot N_S}{T_{RCD}} + \bar{I}_B \qquad (3)$$

C. Modeling Processing Energy Consumption

A vibration monitoring application is intended to analyze the frequency content of the acceleration signals acquired from a vibrating source. As such, a *Fast Fourier Transform* (FFT) is typically used to find the dominant harmonics.

In such case, due to the computational complexity of the algorithm, the FFT computation is the main contribution to the processing energy consumption.

To come up with a valid model, it is important to identify the functional behavior related to a selected control parameter. The FFT implementation has a well known $Nlog(N)$ complexity. Then, it turns out that the associated energy cost in Eq. (4) should be proportional to this $Nlog(N)$ relation[29]. Thus, when examining the proposed expression given by Eq. (4), the fitting value $\bar{Q}_{OP}$ can be interpreted as an estimation of the average cost per operation, and it depends basically on the technology of the used processor.

$$\bar{I}_{PRC} \cong \frac{\bar{Q}_{OP} \cdot N \cdot log(N)}{T_{RCD}} + \bar{I}_B \qquad (4)$$

D. System Model

Once the main blocks are identified, the full model is built by combining each individual block. In our case study this

---

[1]A record is defined as a sequence of N_S continuous samples.

model is expressed by Eq. (5), which combines the three contributions (2), (3) and (4). A set of control parameters must be selected in order to manage the energy consumption. It this step, it is convenient to differentiate between technological and applications parameters. In Eq. (4), constants α, β, γ and δ only depend on the particular choice of sensor, MCU and radio technologies respectively. Recalling the meaning from the individual contribution, α can be interpreted as the charge per sample $\bar{Q}_S$, β represents the cost per operation $\bar{Q}_{OP}$ of the particular μC, while γ is an estimator of the average charge per message $\bar{Q}_{MSG}$. Finally, δ accounts for the system management contribution I_{SYS}. These constants can be easily modified to evaluate alternative technologies.

In turn, N_{SF}, T_{SYN}, N and T_{RCD} are application parameters that can be tuned in order to meet the power requirements. i.e., once fixed the technology dependent constants, this set of parameters provides the mechanism to adjust the device power consumption. The main parameters involved in network consumption are N_{SF} and T_{SYN}, which are related to the range of the communication and the time between synchronization packets. Although both parameters can be seen as with no-dependency between them, a low N_{SF} (less link budget) can affect the synchronization time requested T_{SYN} (due to packets loss). In this work, as stated in previous section, we fix T_{SYN} to 60 seconds, as an optimal value for typical industrial components.

In terms of sensing and processing, two remarks should be made. First, a record is defined as the process of waking up, taking N_S samples and computing an FFT to analyze them. We assume that the number of points computed by the FFT and the number of samples taken by the ADC are the same $N_S \doteq N$. This means that this parameter affects simultaneously the energy contribution of both sensing and processing tasks. Second, once the number of points to be sampled and analyzed is fixed, the duty-cycled behavior of the application determines the time between records as the determining factor of the average power. Specifically, while the time between records is increased, less power is consumed. Therefore, the time interval between consecutive records determines the time scale for power averaging.

$$\bar{I}_{DEV} = \frac{\alpha\,N}{T_{RCD}} + \frac{\beta\,Nlog(N)}{T_{RCD}} + \frac{\gamma\,2^{N_{SF}}}{T_{SYN}} + \delta \qquad (5)$$

TABLE I
FITTING TECHNOLOGICAL PARAMETERS. (†FROM [29])

Contribution (Fit.)	Parameter	Value	Units
Acquisition (Q_{SMP}) †	α	3.5	$[\mu C]$
Processing (Q_{OP}) †	β	0.3	$[\mu C]$
Network (Radio) (Q_{MSG})	γ	6.1	$[\mu C]$
Network (System)	δ	0.1	$[mA]$

By correctly interpreting Eq. 5, application engineers will be able to make better informed technology-related decisions (both hardware and software) at the design stage, allowing a reduction off the prototyping time which accelerates the *go-to-market* of the product.

Fig. 6 presents a simulation obtained by applying Eq. (5)) to different network and recording period configurations. The bars represent the contribution to the energy consumption of the network, sampling and processing components; for different network (spreading factor) and application (record time) settings. Each contribution is computed considering 256, 512 and 1024 samples per record.
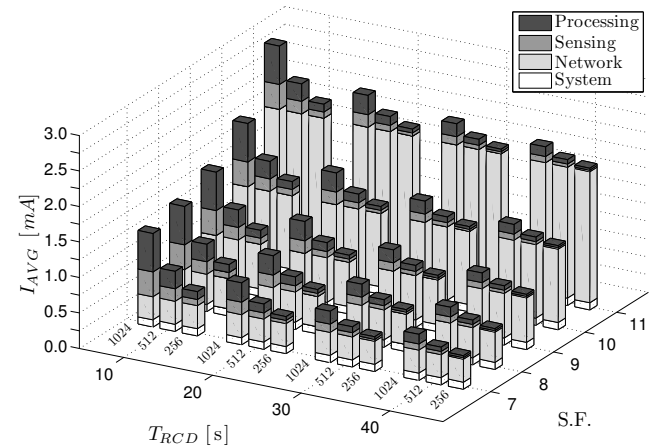

Fig. 6. Contribution of recording interval and network configuration using 256, 512 and 1024 points for the FFT (processing time fixed).

As expected, asymptotic behavior due to the denominator terms can be seen in both axes of Fig. 6. Holding the interval time fixed, the overall energy consumption is reduced when increasing the spreading-factor used in the radio communication. However, the asymptotic decrease limits the amount of energy that can be saved. At a certain point, reducing the spreading-factor (or reducing in some way the energy consumed in the radio communications) does not significantly reduce the average power. Analogously, as the recording interval increases, the energy savings decrease. Hence, this graphical representation serves as a tool to determine which of the parameters yields the highest energy savings once optimized.

IV. HARVESTING DEVICE DIMENSIONING

Once the device power is characterized, a second step is the dimensioning of the energy harvester according to the application requirements. The idea behind harvesting dimensioning is remarkably simple: in the very long term, the energy scavenged from the medium $E_{SCV}(t_\infty)$ must be greater than the energy consumed by the device $E_{DEV}(t_\infty)$ [32]. In practical terms, however, this condition can be relaxed to a more realistic expression:

$$\bar{P}_{SCV} \geq \bar{P}_{DEV} \qquad (6)$$

Yet, in order to apply Eq. (6), two conditions must be satisfied. First, the averaging time window must be long enough to deal with all the short-term variability (running cycles), both at the energy source and at the device side. Second, in a general case, the instantaneous power supplied by the harvester $P_{SCV}(t)$ is independent of the energy consumption rate $P_{DEV}(t)$, and thus they may follow completely different patterns and characteristic periods. The later, mandates a properly sized

energy buffer to absorb the temporary asymmetries between generation and demand [33][34].

In order to meet these two conditions an analysis of the energy source and its variability are fundamental to understand what are the limitations that energy availability imposes to the application.

A. Analyzing the Energy Source

It is a well known fact that solar energy is available intermittently. More concretely, solar irradiation is characterized by a double periodicity: daily cycles (day-night) and seasonal cycles (winter-summer). This double periodicity can be easily appreciated in Fig. 7, where the monthly evolution of solar irradiation in Los Angeles (California) is presented for the 2001-2010 period. This data is publicly available, and similar information can be obtained for other locations [35]. Aside from the monthly evolution, the same figure indicates the day-night variations, which are represented in the vertical direction for each specific month and split into slots of 1 hour.

To make this evolution understandable, data is projected in two orthogonal directions. In the first one, daily irradiation has been aggregated (the figure below the scale-colormap). This plot shows the monthly evolution, i.e., the seasonal variations, averaged per day, for the expected energy income. The second one is a projection of the hourly power of every single month in the period (right side). This figure captures with a single snapshot the historic daily behavior of solar irradiation. Obviously, some months have longer days than others, and even the same month can see irradiation change from one day to another; but the interruption of energy production at night is inevitable.

In light of these patterns, this proposal handles the double periodicity in two different ways: seasonal variations are absorbed by dynamically adapting the application to the expected energy income, while daily energy over-production is stored in a super-capacitor for powering the system at night. The next two sections lay out the procedure in detail.

B. Harvester Sizing and Adaptive Operation

When the available energy is highly variable (as solar irradiation is) the selection of a suitable combination of the harvester size and application settings is complex, as the system should be designed to stay alive even in worst case conditions. This becomes especially relevant when the application needs to dynamically adapt to new, non-predicted conditions, while still remaining energetically self-sustainable.

Looking at the historic evolution of the averaged irradiation (Fig. 7, bottom), the minimum expected value for the daily average power is $0.1 \ kW/m^2$, corresponding to the worst winter period on the record [2]. Based on this observation, and considering the efficiency of the selected solar panel technology (typically $\eta_{Panel} \approx 15{-}25\%$ [36]) and the DC-DC converter ($\eta_{dc} \approx 80{-}85\%$ for off-the-shelf low-cost technologies [37]), it can be expected that the power production per area unit of the system can be estimated in $\hat{P} \approx 0.8 \ mW/cm^2$. This value

corresponds to $\hat{I}_{SCV}{=}0.32 \ mA/cm^2$ once converted to 2.5V (with the losses due to DC/DC conversion accounted for in the efficiency factor η_{dc}).

With this value in mind, the next step is to understand the current requirements of the application. Fig. 8 shows the operational regions for different network configurations (different schedules that can provide different levels of QoS or bandwidth). Typically, the spreading-factor's value is fixed once the network has been deployed. Therefore, a more suitable control parameter is the time between consecutive measurements, which can be varied according to energy availability.

At this point, a key aspect to consider is the asymptotic behavior of Eq. (5). Even when using the very high values of T_{RCD}, the offset term due to network maintenance and system background functionality makes it almost impossible to obtain further energy savings. This is the asymptotic limit below $0.5 \ mA$, which is noticeable in Fig. 8a. It is important to understand that this value is a system limit fixed by the technology used. Therefore, it determines the absolute minimum size of the solar panel, meaning that the harvested current must be above this value in worst case conditions. This is a good example of the necessity for a system-wide view in the wireless device's design flow: a power condition is imposed by radio technology and emerges as a mechanical system constraint through the size of the solar panel.

Bearing in mind the minimum value needed to operate the network, and recalling that expected current per unit are is $\hat{I}_{SCV} \approx 0.3 \ mA/cm^2$, a small form-factor panel of $2cm^2$ guarantees a current of $I_{SCV} = 0.6 \ mA$ in worst case irradiation periods. Then, when the input is beyond this value, the system can keep track of the variations of the energy scavenged and estimate the current income for the next cycle, in order to operate in a more aggressive power mode according to the season.

Following with the example, in Fig. 8a the gray areas represent the feasible zones that satisfy the sustainability condition Eq. (6). In the figure, the device is configured in a low-power mode during winter ($I_{SCV}^{(min)} \simeq 0.6mA$). In this mode, the device analyzes the state of the tower every 30 seconds, which satisfies the sustainability condition for a current of $I_{DEV} \le 0.6mA \le I_{SCV}$ (in the direction of top-left arrow). In summer periods, when the expected incoming energy is around 3 times higher ($I_{SCV}^{(min)} \simeq 1.8mA$), the device can be switched to high performance mode. In this mode, the device takes a record every 5 seconds, which is also sustainable for currents above $I_{DEV} \le 1.8mA \le I_{SCV}$ (bottom-right arrow).

Following a similar analysis, Fig. 8b shows the dependence with the number of points of the FFT. Notably, working in winter conditions, using 1024 points has a great impact on the time interval between records. (T_{RCD} changes from $5s$ for $FFT{=}256$ to more than $20s$ for $FFT{=}1024$).

These examples illustrate how to address the problem of sustainability by means of two different approaches, the interval time between measurements and the numerical resolution, both affecting the performance of the system in different ways.
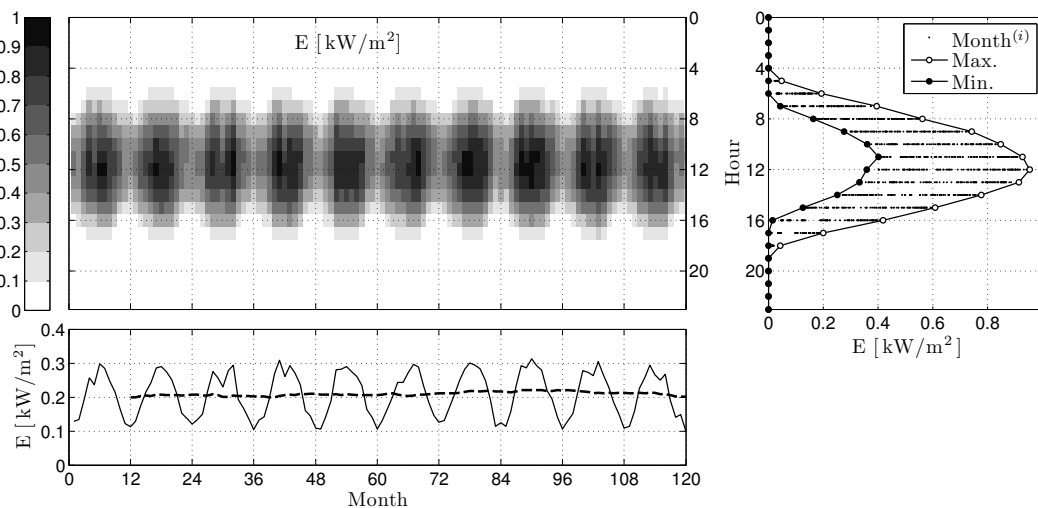
---

[2]This value is roughly 10% of the power received with maximum irradiation

Fig. 7. Solar irradiation in L.A.City along the period 2001-2010.

C. Energy Buffer Sizing

As indicated in the previous section, the validity of Eq. (6) is subject to a proper energy buffer dimensioning. Choosing the capacity of the energy storing device can be accomplished by a careful examination of the energy input and output patterns. When the energy income to the system is available only intermittently, the buffer size is determined by the amount of energy required to operate the device during scarce scavenging periods. In other words, the energy production above the average level during over-production periods ($P_{SCV} > \bar{P}_{DEV}$) has to be buffered in order to power the device when production declines ($P_{SCV} < \bar{P}_{DEV}$).

In our case, night intermittence is managed by temporally buffering to a *super-capacitor* the over-production during the central hours of the day. Super-capacitors support a virtually unlimited number of charge and discharge cycles, therefore making them particularly suitable for this application. One of the drawbacks of super-capacitors is their relatively high self-discharge ratio, but daily replenishment make this effect negligible. In addition, super-capacitor technologies offer a good trade-off between energy density and peak current, the latter being desirable for radio transmissions [38].

For buffering purposes, worst case scenario occurs when the device operate in high performance modes, because the amount of energy to be stored to maintain the system operative at night is required to be higher. So, in opposition to the sizing method, it is important to determine the periods when the maximum amount of harvested energy is expected.

Fig. 9 shows the historic irradiation from Fig. 7 mapped onto the power generated by a $2cm^2$ cell (as measured after the DC/DC regulator). In the high performance settings, the average demand from the device is close to $4.5\ mW$ ($1.8mA$ at $2.5V$). Daytime over-production is depicted with the light grey area inside the maximum production (black-solid dots) and the device demand (dashed-line). This area must be stored for use during the under-production periods, indicated by the dark grey area. In this example, the amount of energy to be buffered is $E_{Buff} \approx 58\ mWh$, which requires a $75\ F$ super-

capacitor [39]. Specifically, we use the Maxwell BCAP0100 with a capacity of 100F in $17cm^3$ (L=45mm d=22mm), used at 75% of its capacity

This result demonstrates how solar harvesting and super-capacitor technologies can be combined into a reduced form factor that enables reasonably small perpetual devices.

V. CONCLUSION

This article addresses the convergence of energy scavengers with industrial wireless sensing and actuating applications. Through a representative application scenario for typical industrial settings, it proposes an analytical model as a tool to facilitate the dimensioning and scavenger selection at pre-deployment stages considering specific application requirements. This approach aims to provide concise answers to the main concerns about energy harvesting and its suitability.

The presented method is applicable to a wide range of use cases, and is defined by the following steps: 1) determine the source of energy in your scenario; 2) determine the duty-cycle and the magnitude of the available energy; 3) simulate within the boundaries of the application variables; 4) select a scavenger dimensioned accordingly to the available energy and an initial estimation of the energy consumption of the application; 5) optimize the application variables and variability taking into account the selected scavenger; and 6) dimension energy buffers to cope with dynamic energy peaks.

Therefore, given an industrial application using a wireless industrial network, and knowing its radio technology, sampling and processing requirements, an accurate estimation of energy demands can be used to determine what scavenger and super-capacitor is required to make it self-sustainable. Furthermore, the parametrized model can be used to properly configure the application, enable different modes of operation in case of varying requirements, e.g., more energy during certain hours may enable more data or processing.

ACKNOWLEDGMENT
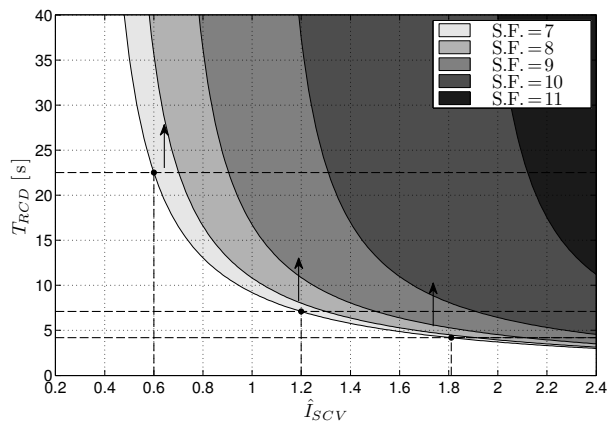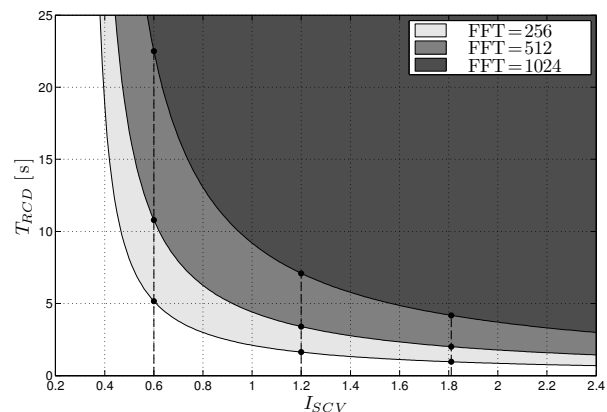
(a) Variable SF

(b) Variable FFT

Fig. 8. Dependence of the time between records and the harvester current for different application configurations. Gray areas represent the feasible zones that satisfy the condition $I_{DEV} \leq I_{SCV}$. The system operates from a low-power mode in winter to a max-performance mode in summer.

Fig. 9. Month-Daily-Hourly variations period 2001-2010. Solid lines represent average for each year.

REFERENCES

[1] P. C. Evans and M. Annunziata, "Industrial internet: Pushing the boundaries of minds and machines," in *White Paper - www.ge.com*, Nov 2012.

[2] M. Palattella, N. Accettura, X. Vilajosana, T. Watteyne, L. Grieco, G. Boggia, and M. Dohler, "Standardized protocol stack for the internet of (important) things," *Communications Surveys Tutorials, IEEE*, vol. 15, pp. 1389–1406, Third 2013.

[3] X. Vilajosana, P. Tuset-Peiro, F. Vazquez-Gallego, J. Alonso-Zarate, and L. Alonso, "Standardized low-power wireless communication technologies for distributed sensing applications," *Sensors*, vol. 14, no. 2, pp. 2663–2682, 2014.

[4] P. Thubert, T. Watteyne, M. R. Palattella, X. Vilajosana, and Q. Wang, "Ietf 6tsch: Combining ipv6 connectivity with industrial performance," in *Innovative Mobile and Internet Services in Ubiquitous Computing (IMIS), 2013 Seventh International Conference on*, pp. 541–546, IEEE, 2013.

[5] J. Yick, B. Mukherjee, and D. Ghosal, "Wireless sensor network survey," *Computer Networks*, vol. 52, no. 12, pp. 2292 – 2330, 2008.

[6] V. Gungor and G. Hancke, "Industrial wireless sensor networks: Challenges, design principles, and technical approaches," *Industrial Electronics, IEEE Transactions on*, vol. 56, pp. 4258–4265, Oct 2009.
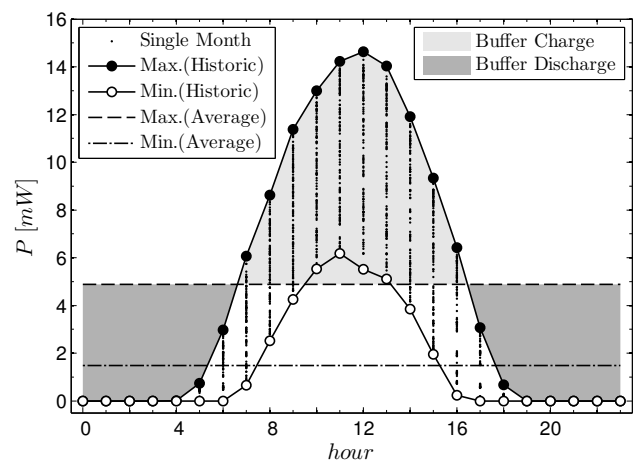
[7] L. Catarinucci, D. De Donno, L. Mainetti, L. Palano, L. Patrono, M. Stefanizzi, and L. Tarricone, "An iot-aware architecture for smart healthcare systems," *Internet of Things Journal, IEEE*, vol. PP, no. 99, pp. 1–1, 2015.

[8] A. Zanella, N. Bui, A. Castellani, L. Vangelista, and M. Zorzi, "Internet of things for smart cities," *Internet of Things Journal, IEEE*, vol. 1, pp. 22–32, Feb 2014.

[9] L. Atzori, A. Iera, and G. Morabito, "The internet of things: A survey," *Computer Networks*, vol. 54, no. 15, pp. 2787 – 2805, 2010.

[10] D. Bandyopadhyay and J. Sen, "Internet of things: Applications and challenges in technology and standardization," *Wireless Personal Communications*, vol. 58, no. 1, pp. 49–69, 2011.

[11] R. Vullers, R. Schaijk, H. Visser, J. Penders, and C. Hoof, "Energy harvesting for autonomous wireless sensor networks," *Solid-State Circuits Magazine, IEEE*, vol. 2, pp. 29–38, Spring 2010.

[12] "802.15.4e-2012: IEEE Standard for Local and metropolitan area networks–Part 15.4: Low-Rate Wireless Personal Area Networks (LR-WPANs) Amendment 1: MAC sublayer," 16 April 2012.

[13] "WirelessHART Specification 75: TDMA Data-Link Layer," 2008. HCF_SPEC-75.

[14] ISA, "ISA-100.11a-2011: Wireless Systems for Industrial Automation: Process Control and Related Applications," May 2011.

[15] D. Miorandi, S. Sicari, F. De Pellegrini, and I. Chlamtac, "Internet of things," *Ad Hoc Netw.*, vol. 10, pp. 1497–1516, sep 2012.

[16] L. D. Xu, W. He, and S. Li, "Internet of things in industries: A survey," *Industrial Informatics, IEEE Transactions on*, vol. 10, pp. 2233–2243, Nov 2014.

[17] J. Stankovic, "Research directions for the internet of things," *Internet of Things Journal, IEEE*, vol. 1, pp. 3–9, Feb 2014.

[18] L. Doherty, W. Lindsay, and J. Simon, "Channel-specific wireless sensor network path data," in *ICCCN*, pp. 89–94, IEEE, 2007.

[19] P. Thubert, T. Watteyne, M. Palattella, X. Vilajosana, and Q. Wang, "Ietf 6tsch: Combining ipv6 connectivity with industrial performance," in *Innovative Mobile and Internet Services in Ubiquitous Computing (IMIS), 2013 7th Int. Conf. on*, pp. 541–546, July 2013.

[20] A. Kansal, J. Hsu, S. Zahedi, and M. B. Srivastava, "Power management in energy harvesting sensor networks," *ACM Transactions on Embedded Computing Systems (TECS)*, vol. 6, no. 4, p. 32, 2007.

[21] R. Torah, P. Glynne-Jones, M. Tudor, T. O'Donnell, S. Roy, and S. Beeby, "Self-powered autonomous wireless sensor node using vibration energy harvesting," *Measurement Science and Technology*, vol. 19, no. 12, p. 125202, 2008.

[22] Semtech Corporation, "SX1272/3/6/7/8 LoRa modem design guide," 2013.

[23] A. Muszynska, "Vibrational diagnostics of rotating machinery malfunctions," *International Journal of Rotating Machinery*, vol. 1, no. 3-4, pp. 237–266, 1995.

[24] J. Brownjohn, "Structural health monitoring of civil infrastructure," *Philosophical Transactions of the Royal Society of London A: Mathematical, Physical and Engineering Sciences*, vol. 365, no. 1851, pp. 589–622, 2007.

[25] F. Rimmer, "Transmission line operations and maintenance," *Electric Energy Magazine*, April 2005.

[26] T. Yin, H. Lam, H. Chow, and H. Zhu, "Dynamic reduction-based structural damage detection of transmission tower utilizing ambient vibration data," *Engineering Structures*, vol. 31, no. 9, pp. 2009 – 2019, 2009.

[27] M. Perez Martinez and L. Gil, "Mètodo y sistema de evaluación de la integridad estructural de torres de celosìa o reticuladas," 09 2013.

[28] Q. Wang, M. Hempstead, and W. Yang, "A realistic power consumption model for wireless sensor network devices," in *Sensor and Ad Hoc Communications and Networks, 2006. SECON '06. 2006 3rd Annual IEEE Communications Society on*, vol. 1, pp. 286–295, 2006.

[29] B. Martinez, X. Vilajosana, F. Chraim, I. Vilajosana, and K. Pister, "When scavengers meet industrial wireless," *Industrial Electronics, IEEE Transactions on*, vol. 62, pp. 2994–3003, May 2015.

[30] X. Vilajosana, Q. Wang, F. Chraim, T. Watteyne, T. Chang, and K. Pister, "A realistic energy consumption model for TSCH networks," *Sensors Journal, IEEE*, vol. 14, pp. 482–489, Feb 2014.

[31] D. Stanislowski, X. Vilajosana, Q. Wang, T. Watteyne, and K. Pister, "Adaptive synchronization in ieee802.15.4e networks," *Industrial Informatics, IEEE Transactions on*, vol. 10, pp. 795–802, Feb 2014.

[32] D. Gunduz, K. Stamatiou, N. Michelusi, and M. Zorzi, "Designing intelligent energy harvesting communication systems," *Communications Magazine, IEEE*, vol. 52, pp. 210–216, January 2014.

[33] K. Tutuncuoglu and A. Yener, "Optimum transmission policies for battery limited energy harvesting nodes," *Wireless Communications, IEEE Transactions on*, vol. 11, pp. 1180–1189, March 2012.

[34] N. Bui and M. Rossi, "Staying alive: System design for self-sufficient sensor networks," *CoRR*, vol. abs/1310.7717, 2013.

[35] "National renewable energy laboratory," 2013.

[36] M. A. Green, K. Emery, Y. Hishikawa, W. Warta, and E. D. Dunlop, "Solar cell efficiency tables (version 44)," *Progress in Photovoltaics: Research and Applications*, vol. 22, no. 7, pp. 701–710, 2014.

[37] A. R. Reisi, M. H. Moradi, and S. Jamasb, "Classification and comparison of maximum power point tracking techniques for photovoltaic system: A review," *Renewable and Sustainable Energy Reviews*, vol. 19, pp. 433–443, 2013.

[38] V. Boicea, "Energy storage technologies: The past and the present," *Proceedings of the IEEE*, vol. 102, pp. 1777–1794, Nov 2014.

[39] A. Pernia, S. Menendez, M. Prieto, J. Martinez, F. Nuno, I. Villar, and V. Ruiz, "Power supply based on carbon ultracapacitors for remote supervision systems," *Industrial Electronics, IEEE Transactions on*, vol. 57, pp. 3139–3147, Sept 2010.

Marius Monton has a PhD in Computer Science by Universitat Autònoma de Barcelona (UAB). From 2004 to 2011 he was member of the Hardware-Software Prototypes and Solutions Lab in Microelectronics department in the UAB. Màrius also was working with GreenSocs from 2007 to 2010 in different projects related to SystemC and TLM modelling, focusing on Virtual Platform design. Màrius joined WorldSensing in 2010 to manage R&D department. He is assistant professor at UAB Engineering School and Co-founder of IoT Partners, an IoT consulting company born in 2015.

Ignasi Vilajosana is the CEO of Worldsensing and Endeavor Entrepreneur; he has strong experience in all stages of company start-up and development. Ignasi has over 10 years of experience in the geophysical sector. He holds a PhD in Physics where he has authored numerous high impact publications. He also has a strong background in signal processing, parametric models and advanced filtering techniques.

Xavier Vilajosana, entrepreneur and co-founder and CIO of Worldsensing. He is also associate professor at the Open University of Catalonia (UOC). From January 2012 to January 2014, Xavier was visiting Professor at the UC Berkeley holding a prestigious Fulbright fellowship. In 2008, he was researcher of France Telecom R&D Labs, Paris. Xavier is one of the main promoters of low power wireless technologies, co-leading the OpenWSN.org initiative at UC Berkeley, and promoting the use of low power wireless standards for the emerging Industrial Internet paradigm. He is also author of different RFCs, as part of his standardization activities for low power industrial networks. He has an MsC degree on Computer Sciences from the Universitat Politècnica de Catalunya (UPC) and a PhD on Computer Science from the UOC. At the moment, he holds 12 patents and more than 25 high impact journal publications.

Borja Martinez received a BSc in Physics and Electronics Engineering, an MSc in Microelectronics and a PhD in Computer Science from the Universidad Autónoma de Barcelona (UAB), Spain. His research interests primary include low power techniques for smart wireless devices, energy efficiency and algorithms. Since 2005, he has been Assistant Professor with the Department of Microelectronics and Electronic Systems, UAB. In 2011 he joined Worldsensing R&D team.